Surg Radiol Anat
DOI 10.1007/s00276-008-0388-4

ORIGINAL ARTICLE

Quantified relationships of the radial nerve with the radial groove and selected humeral landmarks

S. Van Sint Jan · D. Nguyen Van · M. Rooze

Received: 26 December 2007 / Accepted: 2 July 2008

Abstract Anatomical relationships between the radial nerve, the deltoid muscle insertions and several bony landmarks have been investigated to assess the feasibility of surgical transfer of the deltoid transfer during humeral osteotomy. Eleven embalmed human specimens were dissected. Each specimen included the whole thorax, both shoulders and upper limbs. Spatial position of the radial nerve along the radial groove, the deltoid muscle, and several anatomical landmarks was digitised using a three-dimensional (3D) digitiser. Sixteen distances and one angle characterizing the relationships between the path of the radial nerve and the landmarks were processed. Results showed that the average distance between the emergence of the radial nerve from the lateral intermuscular septum and the most distal insertion point of the deltoid muscle on the humeral bone shaft was 47.6 ± 18.5 mm. The angle between a line extending from the entry of the radial nerve into the radial sulcus and its point of emergence (REN–REM line), and on the other hand a line running from the radial emergence and the deltoid muscle tip (REM–DELTIP line) was in average $23.5 \pm 6.7°$. The length of four lines running perpendicular to REM–DELTIP and crossing each quarter of the REN–REM line were interpolated. The length of these four lines was, from proximal to distal, 31.3 ± 11.5 mm; 23.0 ± 7.8 mm; 16.5 ± 6.2 mm; and 7.6 ± 2.6 mm, respectively. These results described in a quantitative way the path of the radial nerve in respect to the humeral bone and the deltoid muscle. These data will be used for further development of a humeral osteotomy protocol taking into account the spatial position of the radial nerve to orientate safely the surgical tools used to cut the humeral shaft.

Keywords Radial nerve · Humeral diaphysis · Surgical approach · Osteosynthesis

Introduction

The anatomy of both radial nerve and deltoid muscle is described in most anatomical textbooks [4, 5, 8, 10]. However, to the authors' knowledge, the detailed relationships between both above structures and the surrounding skeleton have not been previously quantified. Moreover, the radial nerve may be damaged during surgical procedures performed on the posterior aspect of the humeral shaft, for example, in some patients external humeral fixation could provoke radial paralysis [1]. The radial groove is also described as being the main compression location of the radial nerve and a potential source of lesion [9]. Because of the above clinical observations, a better quantification of the radial nerve relationships with the radial groove was justified. Depth of the radial nerve in the soft tissue of the upper arm has been previously quantified using ultrasound [3]. Spatial location of the nerve compared to palpable anatomical landmarks, however, was not found from the literature.

This study aimed to collect quantitative knowledge about the relationships of the radial nerve, the deltoid muscle and several anatomical landmarks. The results will

S. Van Sint Jan (✉) · M. Rooze
Laboratory of Anatomy, Biomechanics and Organogenesis (CP 619), Faculty of Medicine, Université Libre de Bruxelles (ULB), Lennik Street, 808, 1070 Brussels, Belgium
e-mail: sintjans@ulb.ac.be

D. Nguyen Van
Department of Anatomy,
University Training Center For Health Care Professionals (UTCHCP), Ho Chi Minh City, Vietnam

be used as an anatomical basis to develop, in a further research, safety guidelines within surgical protocols related to transfer of the deltoid muscle attachment on the humeral shaft, and humeral osteosynthesis.

Materials and methods

Dissection procedure

Both shoulders and upper arms of 11 embalmed human specimens (all above 60 year-old, no visible musculo–skeletal disorders) were dissected. All dissections were performed by well-trained senior anatomists (Fig. 1). Both skin and subcutaneous tissue were detached to uncover the muscles of the shoulder and arm [2]. The deltoid muscle was further dissected to observe its attachments on the humeral bone. The long head of the triceps brachii muscle was cut close to its origin on the scapula in order to expose the radial nerve. The latter was observable on the anterior aspect of the distal tendon of the latissimus dorsi muscle and ran towards the entry of the radial sulcus. The point, where the nerve was in contact with the bone, was labelled as the radial nerve entry (REN). On the lateral aspect of the upper arm, both brachialis muscle and brachioradialis muscles were dissected to observe the spot where the radial nerve runs through the lateral intermuscular septum. This particular spot was labelled as the radial nerve emergence (REM). Eventually, the lateral head of the triceps brachii was further dissected to observe the radial nerve running in its groove on the posterior aspect of the humeral shaft.

Four anatomical bony landmarks were of interest for this study: the most distal insertion, or apex, of the deltoid muscle on the humeral shaft (DELTIP), the centre of the medial epicondyle (MCON), the centre of the lateral epicondyle (LCON), and the acromial angle (AA) (Fig. 2). Detailed landmark descriptions had to be used in this paper. Indeed, for example the anatomical concept "lateral epicondyle" refers to a relatively broad bony area and not to a punctual spot. Using this landmark within quantitative study required a finer and stricter description of the bony spot to be used. Strict definitions for the above landmarks were previously proposed [12] and used in this paper. Using strict landmark definitions allow performing measurements in a standardized and reproducible manner, and therefore should increase the repeatability of the results [13].

Measurement procedure

During measurements, each specimen was in lateral decubitus with the upper arm aligned in neutral position along the trunk. The upper limb was rigidly attached to the experimental bench using strapping. Digitising was performed using a commercial 3D digitiser (Faro arm®, USA, constructor accuracy: 0.1 mm) that were also rigidly attached on the experimental bench. The real precision of the measurements depends of the actual experimental settings. Previously published results indicated that the experimental digitizing protocol used for this paper showed a precision of 0.8 ± 0.5 mm [11]. Spatial locations of the above-defined anatomical landmarks (AA, DELTIP, REN, REM, LCON, MCON) were digitised in the same reference system.

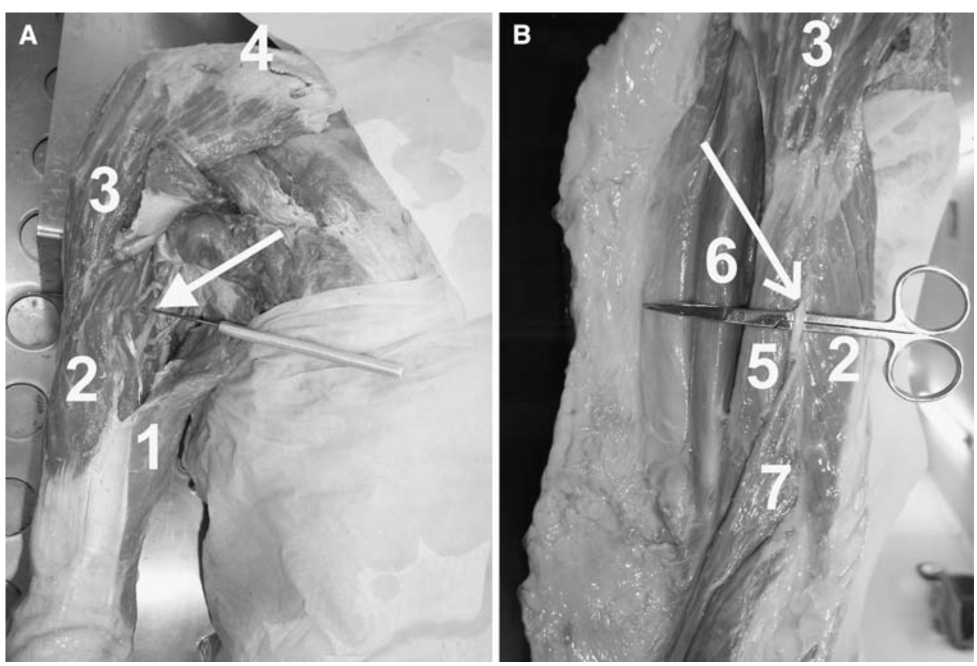

Fig. 1 Dissection of one of the specimen (*left shoulder*). **a** radial nerve entry point (*posterior view*), **b** radial nerve emergence (*lateral view*). *1* long head of triceps brachial muscle, *2* lateral head of triceps brachial muscle, *3* deltoid muscle, *4* acromion, *5* brachialis muscle, *6* biceps brachial muscle, *7* brachoradialis muscle. *Full arrow* radial nerve entry (REN). *Open arrow* radial nerve emergence (REM). See text for explanations

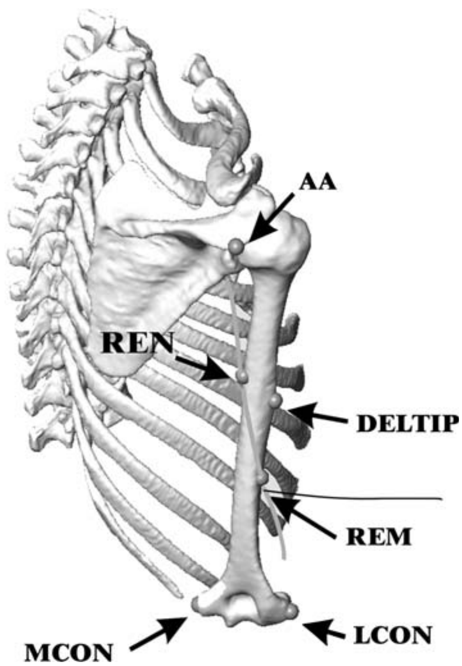

Fig. 2 Schema of the landmarks for dissection and digitisation (illustrated on a virtual 3D bone model obtained from medical imaging). *AA* acromial angle, *REN* radial nerve entry, *REM* radial nerve emergence, *DELTIP* most distal deltoid muscle insertion on humeral shaft, *LCON* lateral epicondyle, *MCON* medial epicondyle

From the above-digitised landmarks several morphological distances and one angle were determined (Fig. 3). All distances were normalized using the MCON–LCON distance to find a ratio between the measured distance and the width of the humeral distal epiphysis.

To interpolate the distances between the REM–DELTIP line and the radial nerve path (i.e., the REN–REM line), the latter was divided into four equal segments (REN–R2, R2–R3, R3–R4, R4–REM). Spatial location of several points (P1, P2, P3, P4) was determined at the intersection of lines perpendicular to the REM–DELTIP line, and starting from each quarter of the REN–REM line. P1 was determined from a line starting from the REN landmark. P2, P3, P4 were determined from lines starting, respectively, from the end of the first (R2), second (R3) and third (R4) quarter of the REN–REM line. The following distances were then determined: DELTIP–P1, DELTIP–P2, DELTIP–P3, DELTIP–P4, REN–P1, R2–P2, R3–P3, R4–P4 and d (=DELTIP–REN–REM).

Results

The mean values for the processed distances and θ angle are given in Tables 1 and 2.

The parameters that are the most relevant for the final applications should be selected among the various values

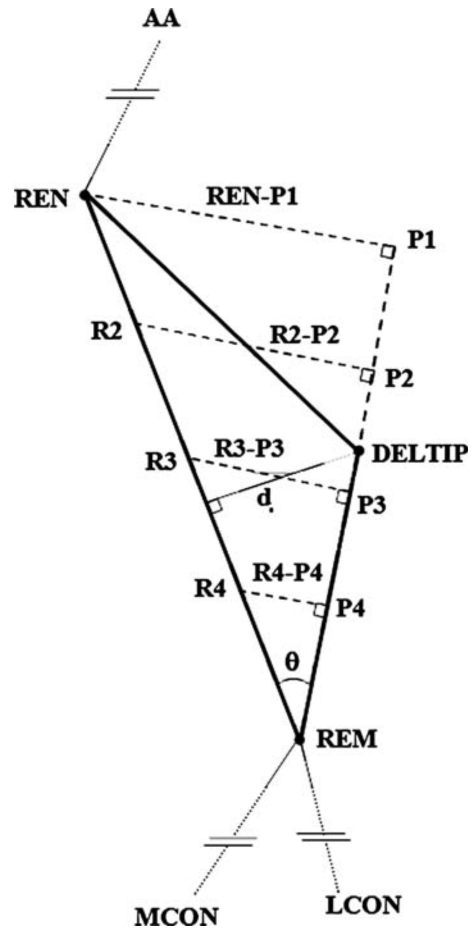

Fig. 3 Determination of distances and angle calculated from the digitised landmarks. *REN–REM* distance between the radial nerve entry and its emergence, *REN–AA* distance between the radial nerve entry and the acromial angle, *REM–LCON* distance between the radial nerve emergence and the lateral epicondyle, *REM–MCON* distance between the radial nerve emergence and the medial epicondyle, *REM–DELTIP* distance between the radial nerve emergence and the deltoid apex, *DELTIP–REN* distance between the deltoid apex and the radial entry, *d = DELTIP–REN–REM* distance between the deltoid apex and the line between both radial entry and radial emergence, θ angle between both REN–REM and DELTIP–REM lines. Algorithms for spatial linear and angular measurements can be found from [6]

found in these tables. An example of application is given in the Discussion section (see below) and illustrates how to estimate the bony area (REN–REM–DELTIP triangle) where the probability of finding the radial nerve is the highest. The authors recommend using the LCON–MCON distance to customize this paper results to a particular patient because these two landmarks are usually easily palpable, even in a surgery room.

Results of this paper indicates that the mean LCON–MCON distance was 61.2 ± 6.4 mm. The distance REM–DELTIP indicates that the REM occurred at a mean distance of 47.6 ± 18.5 mm vertically below the deltoid tip (DELTIP). From REM, the REN point is located in average

Table 1 Distances between the radial nerve landmarks, and DELTIP, MCON and LCON. Results from [7] are also given for comparison

Distance (mm)	In Guse TR. Ostrum RF [7]	This study		
		Mean	SD	Mean (normalized)
LCON–MCON	–	61.2	6.4	–
REN–REM	–	85.9	18.8	1.40
REN–AA	124	123.8	21.4	2.02
REM–LCON	126	97.9	14.6	1.60
REM–MCON	131	108.5	13.1	1.77
REM–DELTIP		47.6	18.5	0.80
DELTIP–REN		52.7	25.3	0.86

Table 2 Angle θ and the distances between the landmarks interpolated on both REN–REM and REM–DELTIP lines

		Mean	SD	Mean (normalized)
Angle (°)	θ	23.5	6.7	–
	DELTIP–P1	33.8	21.0	0.55
	REN–P1	31.3	11.5	0.51
	DELTIP–P2	21.2	22.6	0.35
Distance (mm)	R2–P2	23.0	7.8	0.38
	DELTIP–P3	21.5	24.6	0.35
	R3–P3	16.5	6.2	0.27
	DELTIP–P4	34.1	26.3	0.56
	R4–P4	7.6	2.6	0.12
	d	19.4	10.0	0.32

at 85.9 ± 18.8 mm along the REN–REM line. The mean angle between the REM–DELTIP and the REN–REM lines was 23.5 ± 6.7°.

Discussion

This paper quantified the relationships of the radial nerve running through the radial groove with several anatomical landmarks. All located bony landmarks are strictly defined [12], and readily palpable through soft tissue and visible on 3D patient imaging data if available (see Fig. 2). In-vivo applications of these measurements should therefore be performed to estimate both points of entry and emergence of the radial nerve in and from the radial groove. Normalized measurements presented in this paper can be used during in-vivo applications. The authors advice to measure first the MCON–LCON distance on the patient. Then multiply the result with the normalized mean value of the distance of interest (see Tables 1, 2). These interpolated results allow the estimation of patient-specific values for the parameters quantified in this study.

The distance between the deltoid apex and the emergence of the radial nerve emergence (REM–DELTIP = 47.6 ± 18.5 mm) can be used as an estimation to guide surgical hardware, for example when performing a humeral osteotomy. Using the MCON–LCON ratio the emergence REM should occur at 78% [=(47.6/61.2) × 100] of the MCON–LCON distance distally below the deltoid tip. From REM, the entry point REN can be found by using the REN–REM distance also customized using the MCON–LCON ratio: REN should occur at 140.4% (=(85.9/61.2)*100) of the MCON–LCON distance. The angle θ gives the orientation of the REN–REM line compared to REM–DELTIP; this gives an indication of the nerve orientation, when it emerges from the radial groove, compared to the humeral shaft. The line REM–REN indicates the bony areas where the probability of finding the radial nerve is the highest. These areas should therefore be respected for example during osteosynthesis.

Note that the results presented in this paper are related to a normal elderly population. Some measurements presented could be different, for example when the relationships between the scapula and the humeral bone are abnormal. On the other hand these differences should only be limited to measurements taken between the scapula and the humeral bone (i.e., distance REN–AA). All other parameters are based on landmarks related to the humerus only (medial and lateral epicondyle, deltoid tip, radial sulcus). One can therefore reasonably assume that results for most parameters, but REN–AA, should not be dependent of the position of the humeral head. This should be verified by performing further measurements on pathological shoulders. Another practical problem is the accurate location of some landmarks through the patient soft tissue especially when the patient is obese [13]. This is why the authors advice to use LCON and MCON landmarks because they are usually more easily palpable [12]. Proper palpation training and using the same definition to locate the anatomical landmarks is also advised to guarantee a repeatability of the results [12, 13].

The distances between the REM and both epicondyles (REM–LCON and REM–MCON) found in this study were lower than those reported by Guse and Ostrum [7]. This is probably because we defined the emergence of the radial nerve as the point where the muscle runs through the lateral intermuscular septum on the lateral aspect of the humeral shaft. Unfortunately, Guse and Ostrum [7] do not give any clear definition for that particular point. On the other hand the distance between the acromial angle and the nerve entry is similar (Table 1). The measurement of the angle between the REN–REM line and REM–DELTIP line was 23.5 ± 6.7° (Table 2). This result indicates the orientation of the radial nerve running into the radial grooves compared to the humeral shaft. The five distances (REN–P1, R2–P2, R3–P3, R4–P4 and d) between points of the REN–REM and DELTIP–REM can be used as additional information during surgical intervention involving the radial nerve region. These intervals describe a triangular zone (triangle REN–P1–REM in Fig. 3) in which the probability to find the radial nerve is minimal. Surgery [1] within this zone can be therefore performed in a relatively safe manner. Ultrasound investigation [3] should be facilitated. The outcomes of this paper support the feasibility of a surgical technique dealing with the transposition of the deltoid muscle insertion. The development of this technique is currently under investigation.

Acknowledgments Co-operation between ULB and UTCHCP has been made possible thanks to the support of the University Co-operation for Development of the French-speaking Universities of Belgium (CUD—http://cud.ciuf.be), in collaboration with the Directorate General for International Co-operation of the Belgian Government.

References

1. Chantelot C, Robert G, Aihonnou T et al (2002) Intérêt du fixateur externe dans le traitement des fractures de l'humérus: à propos de 23 fixateurs Orthofix. Chirurgie de la Main 21:134–139
2. Dalcq A, Fautrez J (1947) Manuel théorique et pratique de dissection. Masson, Paris, pp 227–238
3. Foxall G, Skinner D, Hardman J et al (2007) Ultrasound anatomy of the radial nerve in the distal upper arm. Reg Anesth Pain Med 32:217–220
4. Frager J (1946) The anatomy of the human skeleton. J. & A. Churchill Ltd., London, pp 67–68
5. Ger R, Abrahams P (1986) Essentials of clinical anatomy. Pitman, London, p 83
6. Glaeser G (1994) Fast algorithms for 3D-graphics. Springer Verlag, New York, pp 1–22
7. Guse TR, Ostrum RF (1995) The surgical anatomy of the radial nerve around the humerus. Clin Ortho Rel Res 320:149–153
8. Last RJ (1978) Anatomy: Regional and Applied. Churchill Livingstone, Edinburgh London and New York, p 65
9. Lussiez B, Allieu Y (2004) Compression of the radial nerve in the humeral spiral groove (Lotem syndrome). Chirurgie de la Main 23:S102–S109
10. Moore L, Dalley F (2001) Anatomie médicale. De Boeck, Brussels, pp 713–761
11. Sholukha V, Salvia P, Hilal I et al (2004) Calibration and validation of 6 DOF instrumented spatial linkage for biomechanical applications; practical approach. Med Eng Physics 26:251–260
12. Van Sint Jan S (2007) Color atlas of skeletal landmark definitions; Guidelines for reproducible manual and virtual palpations. Churchill Livingstone Elsevier, Edinburgh, pp 50–68
13. Van Sint Jan S, Della Croce U (2005) Accurate palpation of skeletal landmark locations: why standardized definitions are necessary. A proposal. Clin Biomech 20:659–660